Title

Diagnostic advances in synovial fluid analysis and radiographic identification for crystalline arthritis

Journal

Current Opinion in Rheumatology, 31(2)

ISSN

1040-8711

Authors

Zell, Monica
Zhang, Dawen
FitzGerald, John

Publication Date

2019-03-01

DOI

10.1097/bor.0000000000000582

Peer reviewed

Published in final edited form as:

Curr Opin Rheumatol. 2019 March ; 31(2): 134–143. doi:10.1097/BOR.0000000000000582.

Diagnostic advances in synovial fluid analysis and radiographic identification for crystalline arthritis.

Monica Zell, MD[1,*], **Dawen Zhang, MD**[1,*], and **John FitzGerald, MD, PhD**[1]

[1]David Geffen School of Medicine, University of California at Los Angeles, Department of Medicine

Abstract

Purpose of review: This review addresses diagnostic methods for crystalline arthritis including synovial fluid analysis, ultrasound and dual energy CT scan (DECT).

Recent findings: There are new technologies on the horizon to improve the ease, sensitivity and specificity of synovial fluid analysis. Raman spectroscopy uses the spectral signature that results from a material's unique energy absorption and scatter for crystal identification. Lens-free microscopy directly images synovial fluid aspirate on to a complementary metal-oxide semiconductor (CMOS) chip, providing a high-resolution, wide field of view (~20 mm^2) image. Raman spectroscopy and lens-free microscopy may provide additional benefit over compensated polarized light microscopy (CPLM) synovial fluid analysis by quantifying crystal density in synovial fluid samples. Ultrasound and DECT have good sensitivity and specificity for the identification of monosodium urate (MSU) and calcium pyrophosphate (CPP) crystals. However, both have limitations in patients with recent onset gout and low urate burdens.

Summary: New technologies promise improved methods for detection of MSU and CPP crystals. At this time, limitations of these technologies do not replace the need for synovial fluid aspiration for confirmation of crystal detection. None of these technologies address the often concomitant indication to rule out infectious arthritis.

Keywords

Synovial fluid analysis; crystalline arthritis; monosodium urate; calcium pyrophosphate; dual energy CT

Introduction:

Demonstration of monosodium urate (MSU) and calcium pyrophosphate (CPP) crystals in synovial fluid using compensated polarized light microscopy (CPLM) has been the primary

Corresponding author: John FitzGerald, MD, PhD, UCLA Rehabilitation Center, 1000 Veteran Avenue, Room 32-59, Los Angeles, CA 90095-1670, 310-794-5100, jfitzgerald@mednet.ucla.edu.
mzell@mednet.ucla.edu, 310-206-8000
dawenzhang@mednet.ucla.edu, 310-825-2448
*These authors contributed equally to the work.

Conflicts of interest
Dr. FitzGerald is a co-inventor and has patent pending on lens-free microscope.

method of diagnosing gout and calcium pyrophosphate deposition disease (CPPD) since 1969. However, CPLM is infrequently available at point-of-care, particularly outside of rheumatology clinics. User experience and other factors affect the sensitivity and specificity of the methodology, particularly for the smaller, less birefringent CPP crystals. Basic calcium phosphate (BCP) crystals cannot be visualized using CPLM, and reliable methods for identifying them are lacking. Newer methodologies of synovial fluid analysis, including Raman spectroscopy and lens-free microscopy, may improve detection of micro-scale crystals in synovial fluid aspirates. Ultrasound and dual energy CT are non-invasive methods for identifying evidence of MSU crystals and data on utility for identifying CPP crystals are emerging.

Synovial fluid preparation for analysis by compensated polarized light microscopy:

Synovial fluid analysis is ideally performed using freshly aspirated synovial fluid and examination within 24 hours, allowing for observation of intracellular crystals by minimizing cellular decay.[1] However, several studies and a small systematic review[2] have evaluated the impact of synovial fluid storage methods and duration on the stability of MSU and CPP crystal number and morphology.[3–9] These concluded that crystal concentration is better preserved with frozen or refrigerated samples than at room temperature over extended periods of time.[5,8] Crystal morphology is stable and false-positive crystallization generally does not occur.[3] Crystals are stable at room temperature if examined within 1–3 days.[4,9] This is clinically relevant when a synovial fluid sample is initially tested for infection but not crystal analysis; if gram stain and culture are negative, crystal analysis may be requested in the subsequent days. Storage of synovial fluid in vials containing anticoagulants (e.g. heparin or EDTA) provides no benefit in crystal preservation. Sensitivity of MSU[10] and CPP[11] crystal analysis in aspirates with low leukocyte counts can be enhanced by first centrifuging or cytospinning the aspirate to concentrate the particular matters.

Compensated polarized light microscopy:

McCarty and colleagues first introduced CPLM as a method to visualize MSU[12] and CPP[13] crystals in synovial fluid, which has remained the primary technique for the diagnosis of crystal-induced arthropathies over the last fifty years. Recent reviews [14,15] and guidelines [16–18] still consider MSU and CPP crystal identification the gold standard practice for the diagnosis of gout or CPPD, respectively. However, multiple reports suggest that CPLM has variable reliability as a diagnostic tool in the clinical setting,[19,20] with poor inter-rater reliability,[21–24] sensitivity and specificity,[25] particularly for the identification of CPP crystals, which are smaller and less birefringent than MSU crystals. Some of these difficulties stem from inherent challenges of the microscopic system itself. For example, the concentration of crystals necessary for CPLM detection may be higher than clinically relevant in vivo crystal concentrations.[25] CPLM visualizes crystals larger than 1 micrometer, meaning it may not detect very small crystals.[26,27] MSU crystals are typically 10 um in length (range 1 – 20 um) [28]. CPP crystals are smaller with median

length of 3.7 μm for rods (range, 1 – 10 μm) and for rhomboids, median lengths of long and short diagonals of 3.0 and 2.4 μm [29]. In the case of CPP crystals, identification by CPLM is further challenging as up to 20% may be nonbirefringent.[30] Experience with CPLM plays a large role, as one study demonstrated that accuracy of CPLM interpretation improves with examiner training,[31] supporting the call for further synovial fluid analysis training for rheumatology trainees and professionals.[32] While many of the above reports are from over ten years ago, a recent study by Berendsen et al.[33] highlighted the lack of progress in examiner competence in CPLM crystal identification. One hundred and ten highly motivated participants (rheumatologists, laboratory technicians, rheumatology trainees, and other physicians worldwide) with interest in crystal arthritis and diagnosis completed an online test of their ability to interpret CPLM images. Participants were asked to identify 30 images photographed from pathognomonic slides containing different types of crystals or artifacts. The primary outcome, which was the correct identification of all 8 MSU and all 8 clinically important non-MSU images, was achieved by only 39%. Whereas the correct identification of all MSU images was achieved by 81%, only 68% correctly identified all CPP crystals. While this study did not test the participants' real-time microscopy and synovial fluid handling skills, these results underscore the persistent gap in crystal identification proficiency using CPLM.

Alizarin Red Staining:

There remains a lack of any reliable method for the detection of BCP crystals. Due to submicroscopic size (typically less than 1 micrometer as individual crystals), the amorphous appearance of BCP clumps easily mistaken for artifacts or debris, and their non-birefringence, CPLM is an inadequate method for BCP crystal detection.[34] Alizarin red staining is a long-known technique[35] that uses the formation of a red chelation complex between calcium and alizarin to detect calcium-containing compounds. However, different calcium-containing compounds cannot be distinguished by the staining, thus CPP and BCP crystals must be discriminated based on morphologic aspects. While the sensitivity of Alizarin red staining depends on both the pH of the solution and concentration of the dye, there is considerable overlap in the optimal pH and dye concentration ranges for CPP and BCP detection.[34,36] Alizarin red dye must be freshly prepared to the appropriate concentration and pH before it can be added to the synovial fluid sample, complicating the practical use of this technique.

Raman Spectroscopy:

Raman spectroscopy (RS) is a powerful analytic tool with ample research and biologic applications due to its capacity to measure the chemical composition of a sample with 100% specificity.[37] The technique utilizes the principal that each material has an inherent absorption and light scatter when exposed to energy, producing a unique signature or "Raman spectrum". RS can be performed in vivo, without synovial fluid aspiration, or ex vivo on synovial fluid aspirates. While RS was first used in a research setting to identify MSU[38] and CPP[39] crystals utilizing laborious methods, Akkus and colleagues have advanced the use of this technique towards a more clinically feasible approach to MSU and CPP crystal detection.[40–42] To achieve this goal, they developed a protocol to improve

crystal extraction by digesting hyaluronic acid and organic debris in synovial fluid, allowing for a concentrated target of crystals for “point-and-shoot” RS rather than extensively searching for individual crystals [40]. The group then laid the foundation for bringing RS from the research bench to the clinic by a) developing a disposable syringe-filtration technique for crystal isolation and concentration, b) downsizing the system to a less expensive, shoebox-sized apparatus, and c) developing an automated data acquisition and processing protocol for the spectral identification of crystals[41]. The novel shoebox-sized point-of-care RS system (POCRS) can detect MSU and CPP crystals at clinically relevant concentrations of 0.1 microgram/mL and 1 microgram/mL, respectively.

Akkus and colleagues recently evaluated the performance of their POCRS technique compared to CPLM for the detection of MSU and CPP crystals in 174 synovial fluid samples.[42] (See Figure 1) Presence or absence of characteristic spectral peaks for MSU and CPP was used to determine the presence or absence of these crystals using POCRS. The study found notably high overall concordance between POCRS and CPLM (89.7%), with stronger agreement for the detection of MSU crystals than for CPP crystals (kappa coefficients (95% CI) of 0.84 (0.75–0.94) and 0.61 (0.42–0.81), respectively). However, 8 MSU-positive samples were detected by CPLM but not POCRS, which were confirmed as POCRS false negative findings by research-grade (non-point-of-care) RS. POCRS was better at detecting CPP crystals than CPLM: 22 CPP-positive samples were identified by POCRS versus 12 by CPLM, with only one POCRS false negative. Akkus and colleagues concluded that POCRS should not be a replacement for but in conjunction with CPLM, particularly in situations where a trained microscopist is not available or when there is high index of suspicion but ambiguity in crystal identification; a recent systematic review also recommended this strategy [43]. Rosenthal and Pascual’s editorial of the study[44] elegantly reviewed some of the method’s potential advantages, including the ability to measure crystal concentrations in synovial fluid and increased accuracy of crystal identification leading to more accurate diagnoses. Currently, little is known about the relationship between crystal concentration and clinical presentation of crystal arthropathies, thus POCRS has the potential to enhance our understanding of a potential relationship. However, POCRS does not provide information on whether crystals are intracellular (phagocytosed by white blood cells) or extracellular due to the processing technique.

Rosenthal and Pascual also highlighted some of the shortcomings of POCRS and areas for future research [44]. While no basic calcium phosphate (BCP) crystals were detected in this study of POCRS, Rosenthal and Pascual postulated that they should be detectable by this method, potentially by modifying the synovial fluid sample preparation. Current limitations of this methodology include the multistep procedure for synovial fluid sample preparation prior to POCRS, and unclear cost and clinical feasibility. Finally, further comparison of POCRS results with conventional confirmatory crystal identification methods will be useful.

Two recent pilot studies examined the ability of RS to detect MSU crystals *in vivo* from the first metatarsophalangeal (MTP) joint using a non-invasive technique in which the Raman spectroscope was placed on the ground to image the medial aspect of the 1st MTP joint. [45,46] While both studies reported detection of several known MSU spectral peaks in known gout patients, there was significant noise interference and overlap with peaks found

in healthy controls, as well as logistical barriers with the noninvasive method. For example, RS was unable to evaluate the dorsal aspect of the 1st MTP joint due to patient and equipment positioning, and therefore false negative results in gout patients may have been due to inability to assess all aspects of the 1st MTP.

Lens-free microscopy:

Lens-free on-chip microscopy has developed over the past decade as a novel detection method with numerous emerging applications in global health, environmental fieldwork, and medical point-of-care settings.[47–49] The lens-free platform setup positions a transparent body fluid sample above a complementary metal-oxide semiconductor (CMOS) image sensor. The minimal sensor-to-sample distance results in a field of view (FOV) multiple orders of magnitude larger than a conventional lens-based microscope, allowing greater efficiency through analysis of a single digital image rather than the need to resample multiple CPLM small FOV. A hologram of the diffracted light pattern from the sample is taken in by an image sensor that utilizes reconstruction algorithms to generate an image of the sample.[50] For the analysis of birefringent crystals, a circular polarizer, λ/4 retardation plate and linear polarizer are added to the setup. (See Figure 2) This polarized microscope can perform wide-field (~20 mm^2) imaging of birefringent objects with sub-micron resolution.[51] The reconstructed holograms show images of MSU and CPP crystals. (See Figure 3) The inexpensive platform and high-resolution wide FOV provides potential advantages over traditional CPLM including point-of-care implementation.

Other methods of crystal identification:

Fourier transform infrared spectroscopy (FTIR) and x-ray diffraction are definitive methods for crystal characterization. [52] However, due to high cost, complex instrumentation and limited availabity outside the research setting they have limited clinical utility. Both techniques exploit the concept that each crystalline material possesses a unique material signature that can be elicited; FTIR evokes a crystal’s inherent infrared wavelength absorption pattern, whereas x-ray diffraction identifies a crystal’s characteristic diffraction pattern of incident x-rays. While these methods were originally included in McCarty’s diagnostic criteria for CPPD, they are not in regular use.[53]

Ultrasound evaluation of crystalline arthropathy:

Ultrasound (US) has become a valuable tool for the identification of MSU and CPP crystals. Crystalline deposition reflects ultrasound waves more intensely than surrounding soft tissues creating several unique ultrasound findings. Some of these findings have high sensitivity and specificity for either MSU or CPP crystals. The double contour sign (DCS) is a hyperechoic band over the superficial margin of cartilage (see Figure 4) and had good sensitivity (60.1%) and high specificity (91.3%) compared to gold-standard presence of MSU crystals identified by CPLM of synovial fluid aspirate in a recent large multicenter study [54]. While there are other US findings suggestive of MSU deposition, DCS is the only ultrasonographic imaging gout sign recognized in the 2015 ACR/EULAR gout classification criteria[16].

Other studies have also supported high specificity (90% range) for DCS [55–57]. However, in patients with gout for less than 2 years, sensitivity (50%) is lower than for patients with established disease ≥ 2 years duration (63%). Still, even in patients with recent disease onset, the positive predictive value (79%) and negative predictive value (77%) for DCS is good. [54] One study noted the median disease duration was 3.5 years in patients with a DCS. Other findings that are useful include US findings of tophus (presence of a hyperechoic, heterogeneous lesion surrounded by an anechoic rim) and “snowstorm” appearance.[54]

CPP crystal intra-hylalan or fibro cartilage deposition can be distinguished from MSU crystal more superficial hyalan cartilage deposition. The OMERACT CPPD Ultrasound Task Force described good intra-reader reliability (kappa = 0.81) and moderately good inter-reader reliability (kappa = 0.66) across various joints [58] with better agreement for the hyaline cartilage and menisci of the knee than other structures of the knee (e.g. synovial fluid or tendon) or other joints (e.g. wrist) [59]. From this effort, they created an atlas to describe the locations (hyaline and fibrocartilage, tendon and synovial fluid) findings for CPP deposition in those regions [58]. Compared to conventional radiography (CR), US detection of CPP deposits has yielded equal or higher sensitivity (60–100%) and similar specificity (85–100%) in wrists, knees, and hips with CPP crystals in synovial fluid as a gold standard [60–63]. Ogdie et al. reported excellent specificity (92.9%) for the DCS for crystal-proven gout compared to crystal-proven CPPD arthropathy controls [54]. However, Löffler et al. reported that it was difficult to distinguish between MSU and CPP deposition at the knees and ankles [64].

Tendon and ligament MSU deposition are also commonly imaged by US. Naredo et al. described 133 patients (91 with gout, 42 with controls) that the MTP1 (57.1%), patello-femoral (intra-articular femoral condyle surface) (41.8%), radiocarpal (38.5%), mid-carpal (28.6%), and knee (25.3%) were the most frequently affected articular surfaces with MSU deposition. Patellar tendon (60.4%), triceps tendon (47.3%), quadriceps (38.%) and Achilles (34.1%) were the most common tendons for MSU deposition[65]. The authors went on to note that imaging beyond the symptomatic joint may increase diagnostic yield. CPP deposition has been reported in the Achilles tendon and plantar fascia with US as well [66,67].

DECT (Dual Energy CT)

In place of a single energy source as used in conventional CT, DECT uses two different energies (80 or 100 kV and 140 kV) at orthogonal angles to each other to gather unique attenuation profiles for targets with varying densities. With post-processing software, low-density urate deposition can be differentiated from other denser materials such as calcium based on spectral profiles. DECT has been widely studied in gout, though distinct post-processing software packages have been developed for MSU as well as CPP crystals. The software assigns different color-codes to materials with different spectral profiles, and presents 3-dimensional renderings where volume of urate deposition can be calculated. (See Figure 5)

Automated volumetric quantification of MSU by software results in very high inter-observer and intra-observer reliability with interclass correlation coefficient (ICC) 0.95–1.00[68,69]. Compared to gold standard MSU identification by CPLM in synovial fluid, DECT sensitivity ranges from 78–100% with a specificity between 76–93% [70–73]. As with US, sensitivity is lower in patients with recent onset gout[70,73]. The sensitivity for detection of MSU is lower in non-tophaceous gout compared to tophaceous gout,[74] which may partially explain the greater sensitivity in patients with longstanding disease. False negatives also occur in lower density targets including MSU positive synovial fluid or bursitis with soluble MSU “liquid tophus” [75]. By correlating DECT with histology, it has been demonstrated that early stage, unconcentrated tophi may be missed by DECT [76]. The limit of detection of DECT is frequently at < 2 mm, so false negatives may occur as microscopic tophi may be missed in the voxel[77].

DECT has been able to image rare locations of urate deposition. A case report described a patient with lumbar radicular symptoms who had extensive tophi seen on DECT in the lumbar intervertebral discs, posterior column, and facet joints. This was confirmed with positive MSU on histology after laminectomy and surgical removal of tophi[78]. Another case report noted a patient with cord compression of a thoracic vertebrae, with improvement of paraparesis after several months of urate lowering therapy[79]. Other novel areas of interest for detection of urate by DECT include the costal cartilages, intervertebral discs, sacroiliac joints, and coronary/aortic vasculature [80–82]. However, Bongartz et al reported false positive DECT signals in patients with severe knee osteoarthritis, and therefore confirmation with future studies is needed to determine if these locations truly represent urate deposition or imaging artifact [70].

A limitation to the widespread use of DECT as tool for routine identification of MSU crystals is that DECT scanners are not widely available. To overcome lack of access to hardware, single source DECT with rapid switching between the 80/100 and 140 kV energies has been studied, but its experience in gout has been limited to date [83].

The ability of DECT to identify CPP crystals has been studied in a radiographic phantom and ex vivo meniscus specimens; in vivo studies have not been published to date. In a small study involving subjects undergoing total knee arthroplasty, compared to gold standard CPP crystal identification in synovial fluid, DECT had a greater sensitivity than conventional radiography (77.8% vs 44.4%) for CPPD detection. Another study found CPPD on DECT co-localized with CPPD on meniscal histology[84]. A case report and a phantom model reported the ability of DECT to distinguish between urate and CPPD, but this requires further study[85,86].

Conclusion:

CPLM of synovial fluid has been the unchallenged diagnostic method for detecting MSU and CPP crystals for 60 years, though alternative methods are gaining scientific validity. Both improved methods of synovial fluid analysis (Raman spectroscopy and lens-free microscopy) and non-invasive methods (ultrasound, DECT, and in vivo Raman spectroscopy) show significant promise. Ultrasound, RS and lens-free microscopy are

relatively inexpensive and could be used for point-of-care diagnosis. However, challenges remain. Ultrasound and DECT are sensitive to sufficient crystal deposition but are less sensitive when needed most (e.g. first clinical presentation of an inflammatory mono-arthritis suspicious for crystalline arthritis). None of these methods currently address the concomitant need to rule out infectious arthritis, but RS and lens-free methodologies could potentially be adapted to address this need.

Acknowledgments

Financial support and sponsorship

Dr. FitzGerald's salary is supported by a grant from the National Institutes of Health (R21AR072946) to evaluate validity of lens-free microscope.

REFERENCES:

1. Pascual E, Sivera F, Andres M: Synovial fluid analysis for crystals. Curr Opin Rheumatol 2011, 23:161–169. [PubMed: 21285711]
2. Graf SW, Buchbinder R, Zochling J, Whittle SL: The accuracy of methods for urate crystal detection in synovial fluid and the effect of sample handling: a systematic review. Clin Rheumatol 2013, 32:225–232. [PubMed: 23138881]
3. de Medicis R, Dansereau JY, Menard HA, Lussier A: [Diagnosis of gout: problems caused by crystallization "in vitro" of sodium urate]. Union Med Can 1979, 108:810, 812, [PubMed: 505657]
4. Bible MW, Pinals RS: Late precipitation of monosodium urate crystals. J Rheumatol 1982, 9:480.
5. Kerolus G, Clayburne G, Schumacher HR, Jr.: Is it mandatory to examine synovial fluids promptly after arthrocentesis? Arthritis Rheum 1989, 32:271–278. [PubMed: 2930602]
6. Galvez J, Saiz E, Linares LF, Climent A, Marras C, Pina MF, Castellon P: Delayed examination of synovial fluid by ordinary and polarised light microscopy to detect and identify crystals. Ann Rheum Dis 2002, 61:444–447. [PubMed: 11959769]
7. Robier C, Neubauer M, Stettin M, Lunzer R, Rainer F: Dried cytospin preparations of synovial fluid are a stable material for long-time storage and delayed crystal analysis. Clin Rheumatol 2012, 31:1115–1116. [PubMed: 22415468]
8. McGill NW, Swan A, Dieppe PA: Survival of calcium pyrophosphate crystals in stored synovial fluids. Ann Rheum Dis 1991, 50:939–941. [PubMed: 1768165]
9. Tausche AK, Gehrisch S, Panzner I, Winzer M, Range U, Bornstein SR, Siegert G, Wunderlich C, Aringer M: A 3-day delay in synovial fluid crystal identification did not hinder the reliable detection of monosodium urate and calcium pyrophosphate crystals. J Clin Rheumatol 2013, 19:241–245. [PubMed: 23872540]
10. Robier C, Stettin M, Quehenberger F, Neubauer M: Cytospin preparations are superior to common smears in the detection of monosodium urate crystals in low-cellular synovial fluids. Clin Rheumatol 2014, 33:1797–1800. [PubMed: 24744156]
11. Robier C, Quehenberger F, Neubauer M, Stettin M, Rainer F: The cytospin technique improves the detection of calcium pyrophosphate crystals in synovial fluid samples with a low leukocyte count. Rheumatol Int 2014, 34:773–776. [PubMed: 23388697]
12. McCarty DJ, Hollander JL: Identification of urate crystals in gouty synovial fluid. Ann Intern Med 1961, 54:452–460. [PubMed: 13773775]
13. Kohn NN, Hughes RE, Mc CD, Jr., Faires JS: The significance of calcium phosphate crystals in the synovial fluid of arthritic patients: the "pseudogout syndrome". II. Identification of crystals. Ann Intern Med 1962, 56:738–745. [PubMed: 14457846]
14. Rosenthal AK, Ryan LM: Calcium Pyrophosphate Deposition Disease. N Engl J Med 2016, 374:2575–2584. [PubMed: 27355536]
15. Dalbeth N, Merriman TR, Stamp LK: Gout. Lancet 2016, 388:2039–2052. [PubMed: 27112094]

16. Neogi T, Jansen TL, Dalbeth N, Fransen J, Schumacher HR, Berendsen D, Brown M, Choi H, Edwards NL, Janssens HJ, et al.: 2015 Gout Classification Criteria: an American College of Rheumatology/European League Against Rheumatism collaborative initiative. Arthritis Rheumatol 2015, 67:2557–2568. [PubMed: 26352873]
17. Newberry SJ, FitzGerald JD, Motala A, Booth M, Maglione MA, Han D, Tariq A, O'Hanlon CE, Shanman R, Dudley W, et al.: Diagnosis of Gout: A Systematic Review in Support of an American College of Physicians Clinical Practice Guideline. Ann Intern Med 2017, 166:27–36. [PubMed: 27802505]
18. Zhang W, Doherty M, Bardin T, Barskova V, Guerne PA, Jansen TL, Leeb BF, Perez-Ruiz F, Pimentao J, Punzi L, et al.: European League Against Rheumatism recommendations for calcium pyrophosphate deposition. Part I: terminology and diagnosis. Ann Rheum Dis 2011, 70:563–570. [PubMed: 21216817]
19. Dieppe P, Swan A: Identification of crystals in synovial fluid. Ann Rheum Dis 1999, 58:261–263. [PubMed: 10225806]
20. Swan A, Amer H, Dieppe P: The value of synovial fluid assays in the diagnosis of joint disease: a literature survey. Ann Rheum Dis 2002, 61:493–498. [PubMed: 12006320]
21. Schumacher HR,, Jr., Sieck MS, Rothfuss S, Clayburne GM, Baumgarten DF, Mochan BS, Kant JA: Reproducibility of synovial fluid analyses. A study among four laboratories. Arthritis Rheum 1986, 29:770–774. [PubMed: 3718565]
22. McGill NW, York HF: Reproducibility of synovial fluid examination for crystals. Aust N Z J Med 1991, 21:710–713. [PubMed: 1759919]
23. von Essen R, Holtta AM, Pikkarainen R: Quality control of synovial fluid crystal identification. Ann Rheum Dis 1998, 57:107–109. [PubMed: 9613340]
24. Hasselbacher P: Variation in synovial fluid analysis by hospital laboratories. Arthritis Rheum 1987, 30:637–642. [PubMed: 3606682]
25. Gordon C, Swan A, Dieppe P: Detection of crystals in synovial fluids by light microscopy: sensitivity and reliability. Ann Rheum Dis 1989, 48:737–742. [PubMed: 2478085]
26. Bjelle A, Crocker P, Willoughby D: Ultra-microcrystals in pyrophosphate arthropathy. Crystal identification and case report. Acta Med Scand 1980, 207:89–92. [PubMed: 6245562]
27. Swan A, Chapman B, Heap P, Seward H, Dieppe P: Submicroscopic crystals in osteoarthritic synovial fluids. Ann Rheum Dis 1994, 53:467–470. [PubMed: 7944620]
28. Paul H, Reginato AJ, Schumacher HR: Morphological characteristics of monosodium urate: a transmission electron microscopic study of intact natural and synthetic crystals. Ann Rheum Dis 1983, 42:75–81. [PubMed: 6830327]
29. Zell M RA, Aung T, Kaldas M, Fitzgerald J: Calcium Pyrophosphate Crystal Size, Shape and Appearance Variability [abstract]. Arthritis Rheumatol 2017, 69
30. Ivorra J, Rosas J, Pascual E: Most calcium pyrophosphate crystals appear as non-birefringent. Ann Rheum Dis 1999, 58:582–584. [PubMed: 10460193]
31. Lumbreras B, Pascual E, Frasquet J, Gonzalez-Salinas J, Rodriguez E, Hernandez-Aguado I: Analysis for crystals in synovial fluid: training of the analysts results in high consistency. Ann Rheum Dis 2005, 64:612–615. [PubMed: 15769916]
32. Schumacher HR, Chen LX, Mandell BF: The time has come to incorporate more teaching and formalized assessment of skills in synovial fluid analysis into rheumatology training programs. Arthritis Care Res (Hoboken) 2012, 64:1271–1273. [PubMed: 22555864]
33. Berendsen D, Neogi T, Taylor WJ, Dalbeth N, Jansen TL: Crystal identification of synovial fluid aspiration by polarized light microscopy. An online test suggesting that our traditional rheumatologic competence needs renewed attention and training. Clin Rheumatol 2017, 36:641–647. [PubMed: 27837341]
34. Yavorskyy A, Hernandez-Santana A, McCarthy G, McMahon G: Detection of calcium phosphate crystals in the joint fluid of patients with osteoarthritis - analytical approaches and challenges. Analyst 2008, 133:302–318. [PubMed: 18299743]
35. Paul H, Reginato AJ, Schumacher HR: Alizarin red S staining as a screening test to detect calcium compounds in synovial fluid. Arthritis Rheum 1983, 26:191–200. [PubMed: 6186260]

36. Shoji K: [Alizarin red S staining of calcium compound crystals in synovial fluid]. Nihon Seikeigeka Gakkai Zasshi 1993, 67:201–210. [PubMed: 7686572]

37. Butler HJ, Ashton L, Bird B, Cinque G, Curtis K, Dorney J, Esmonde-White K, Fullwood NJ, Gardner B, Martin-Hirsch PL, et al.: Using Raman spectroscopy to characterize biological materials. Nat Protoc 2016, 11:664–687. [PubMed: 26963630]

38. McGill N, Dieppe PA, Bowden M, Gardiner DJ, Hall M: Identification of pathological mineral deposits by Raman microscopy. Lancet 1991, 337:77–78. [PubMed: 1670728]

39. Maugars YM, Peru LF, el Messaoudi B, Michaud GO, Berthelot JM, Prost AM, Daculsi G: Pelvic pseudotumoral calcium pyrophosphate dihydrate deposition: an ultrastructural study. J Rheumatol 1994, 21:573–576. [PubMed: 8006907]

40. Cheng X, Haggins DG, York RH, Yeni YN, Akkus O: Analysis of crystals leading to joint arthropathies by Raman spectroscopy: comparison with compensated polarized imaging. Appl Spectrosc 2009, 63:381–386. [PubMed: 19366502]

41. Li B, Yang S, Akkus O: A customized Raman system for point-of-care detection of arthropathic crystals in the synovial fluid. Analyst 2014, 139:823–830. [PubMed: 24419093]

*42. Li B, Singer NG, Yeni YN, Haggins DG, Barnboym E, Oravec D, Lewis S, Akkus O: A Point-of-Care Raman Spectroscopy-Based Device for the Diagnosis of Gout and Pseudogout: Comparison With the Clinical Standard Microscopy. Arthritis Rheumatol 2016, 68:1751–1757. [PubMed: 26882173] Li et al (2016):*This work demonstrates the concordance of point-of-care Raman spectroscopy with gold standard CPLM and its superior detection for CPP crystals.

43. Wu Y, Chen K, Terkeltaub R: Systematic review and quality analysis of emerging diagnostic measures for calcium pyrophosphate crystal deposition disease. RMD Open 2016, 2:e000339. [PubMed: 27933211]

44. Rosenthal AK, Pascual E: Editorial: Decreasing Crystal-Induced Consternation: New Methods of Crystal Identification. Arthritis Rheumatol 2016, 68:1574–1577. [PubMed: 26882418]

45. Curran DJ, Rubin L, Towler MR: Raman Spectroscopy Applied to the Noninvasive Detection of Monosodium Urate Crystal Deposits. Clin Med Insights Arthritis Musculoskelet Disord 2015, 8:55–58. [PubMed: 26327784]

46. Abhishek A, Curran DJ, Bilwani F, Jones AC, Towler MR, Doherty M: In vivo detection of monosodium urate crystal deposits by Raman spectroscopy-a pilot study. Rheumatology (Oxford) 2016, 55:379–380. [PubMed: 26342227]

47. Roy M, Seo D, Oh S, Yang JW, Seo S: A review of recent progress in lens-free imaging and sensing. Biosens Bioelectron 2017, 88:130–143. [PubMed: 27503410]

48. Kim SB, Bae H, Koo KI, Dokmeci MR, Ozcan A, Khademhosseini A: Lens-free imaging for biological applications. J Lab Autom 2012, 17:43–49. [PubMed: 22357607]

49. McLeod E, Ozcan A: Microscopy without lenses. Phys. Today 2017, 70:50–56.

50. Bishara W, Su TW, Coskun AF, Ozcan A: Lensfree on-chip microscopy over a wide field-of-view using pixel super-resolution. Opt Express 2010, 18:11181–11191. [PubMed: 20588977]

51. Zhang Y, Lee SY, Zhang Y, Furst D, Fitzgerald J, Ozcan A: Wide-field imaging of birefringent synovial fluid crystals using lens-free polarized microscopy for gout diagnosis. Sci Rep 2016, 6:28793. [PubMed: 27356625] Zhang et al (2016): This work introduces the lens-free polarized microscope and its high-resolution, wide field of view imaging for point-of-care crystal detection.

52. Rosenthal AK, Mandel N: Identification of crystals in synovial fluids and joint tissues. Curr Rheumatol Rep 2001, 3:11–16. [PubMed: 11177766]

53. Ryan L, McCarty D: Calcium pyrophosphate crystal deposition disease; pseudogout; articular chondrocalcinosis In Arthritis and allied conditions: a textbook of rheumatology, edn 10th Edited by McCarty D: Lea & Febiger; 1985:1515–1546.

54. Ogdie A, Taylor WJ, Neogi T, Fransen J, Jansen TL, Schumacher HR, Louthrenoo W, Vazquez-Mellado J, Eliseev M, McCarthy G, et al.: Performance of Ultrasound in the Diagnosis of Gout in a Multicenter Study: Comparison With Monosodium Urate Monohydrate Crystal Analysis as the Gold Standard. Arthritis Rheumatol 2017, 69:429–438. [PubMed: 27748084] Ogdie et al. 2017 This large, multi-center study of a cohort of patients with features concerning for

crystalline infalmmatory describes sensitivity, specificity and predictive values of ultrasound highlighting that disease duration has an important impact on diagnostic performance.

55. Das S, Ghosh A, Ghosh P, Lahiri D, Sinhamahapatra P, Basu K: Sensitivity and specificity of ultrasonographic features of gout in intercritical and chronic phase. International journal of rheumatic diseases 2017, 20:887–893. [PubMed: 27529533]
56. Elsaman AM, Muhammad EMS, Pessler F: Sonographic Findings in Gouty Arthritis: Diagnostic Value and Association with Disease Duration. Ultrasound Med Biol 2016, 42:1330–1336. [PubMed: 26995154]
57. Naredo E, Uson J, Jimenez-Palop M, Martinez A, Vicente E, Brito E, Rodriguez A, Cornejo FJ, Castaneda S, Martinez MJ, et al.: Ultrasound-detected musculoskeletal urate crystal deposition: which joints and what findings should be assessed for diagnosing gout? Ann Rheum Dis 2014, 73:1522–1528. [PubMed: 23709244]
58. Filippou G, Scire CA, Damjanov N, Adinolfi A, Carrara G, Picerno V, Toscano C, Bruyn GA, D'Agostino MA, Delle Sedie A, et al.: Definition and Reliability Assessment of Elementary Ultrasonographic Findings in Calcium Pyrophosphate Deposition Disease: A Study by the OMERACT Calcium Pyrophosphate Deposition Disease Ultrasound Subtask Force. J Rheumatol 2017, 44:1744–1749. [PubMed: 28250136]
59. Filippou G, Scire CA, Adinolfi A, Damjanov NS, Carrara G, Bruyn GAW, Cazenave T, D'Agostino MA, Delle Sedie A, Di Sabatino V, et al.: Identification of calcium pyrophosphate deposition disease (CPPD) by ultrasound: reliability of the OMERACT definitions in an extended set of joints-an international multiobserver study by the OMERACT Calcium Pyrophosphate Deposition Disease Ultrasound Subtask Force. Ann Rheum Dis 2018, 77:1194–1199. [PubMed: 29535120]
60. Filippou G, Adinolfi A, Cimmino MA, Scire CA, Carta S, Lorenzini S, Santoro P, Sconfienza LM, Bertoldi I, Picerno V, et al.: Diagnostic accuracy of ultrasound, conventional radiography and synovial fluid analysis in the diagnosis of calcium pyrophosphate dihydrate crystal deposition disease. Clin Exp Rheumatol 2016, 34:254–260. [PubMed: 26886247]
61. Forien M, Combier A, Gardette A, Palazzo E, Dieude P, Ottaviani S: Comparison of ultrasonography and radiography of the wrist for diagnosis of calcium pyrophosphate deposition. Joint Bone Spine 2018, 85:615–618. [PubMed: 28965942]
62. Di Matteo A, Filippucci E, Cipolletta E, Musca A, Carotti M, Mashadi Mirza R, Jesus D, Martire V, Pierucci D, Di Carlo M, et al.: Hip involvement in patients with calcium pyrophosphate deposition disease: potential and limits of musculoskeletal ultrasound. Arthritis Care Res 2018.
63. Filippou G, Adinolfi A, Iagnocco A, Filippucci E, Cimmino MA, Bertoldi I, Di Sabatino V, Picerno V, Delle Sedie A, Sconfienza LM, et al.: Ultrasound in the diagnosis of calcium pyrophosphate dihydrate deposition disease. A systematic literature review and a meta-analysis. Osteoarthritis Cartilage 2016, 24:973–981. [PubMed: 26826301]
64. Löffler C, Sattler H, Peters L, Löffler U, Uppenkamp M, Löffler C, Sattler H, Peters L, Löffler U, Uppenkamp M, et al.: Distinguishing Gouty Arthritis from Calcium Pyrophosphate Disease and Other Arthritides Distinguishing Gouty Arthritis from Calcium Pyrophosphate Disease and Other Arthritides. 2015, 42.
65. Naredo E, Uson J, Jiménez-palop M, Martínez A, Vicente E, Brito E, Rodríguez A, Cornejo FJ, Castañeda S, Martínez MJ, et al.: Ultrasound-detected musculoskeletal urate crystal deposition : which joints and what findings should be assessed for diagnosing gout ? 2014:1522–1528.
66. Ellabban AS, Kamel SR, Abo Omar HAS, El-Sherif AMH, Abdel-Magied RA: Ultrasonographic findings of Achilles tendon and plantar fascia in patients with calcium pyrophosphate deposition disease. Clinical rheumatology 2012, 31:697–704. [PubMed: 22203095]
67. Filippou G, Filippucci E, Tardella M, Bertoldi I, Di Carlo M, Adinolfi A, Grassi W, Frediani B: Extent and distribution of CPP deposits in patients affected by calcium pyrophosphate dihydrate deposition disease: an ultrasonographic study. Ann Rheum Dis 2013, 72:1836–1839. [PubMed: 23532170]
68. Choi HK, Burns LC, Shojania K, Koenig N, Reid G, Abufayyah M, Law G, Kydd AS, Ouellette H, Nicolaou S: Dual energy CT in gout: a prospective validation study. Ann Rheum Dis 2012, 71:1466–1471. [PubMed: 22387729]

69. Dalbeth N, Aati O, Gao A, House M, Liu Q, Horne A, Doyle A, McQueen FM: Assessment of tophus size: a comparison between physical measurement methods and dual-energy computed tomography scanning. Journal of clinical rheumatology : practical reports on rheumatic & musculoskeletal diseases 2012, 18:23–27. [PubMed: 22157268]
70. Bongartz T, Glazebrook KN, Kavros SJ, Murthy NS, Merry SP, Franz WB, 3rd, Michet CJ, Veetil BM, Davis JM, 3rd, Mason TG, 2nd, et al.: Dual-energy CT for the diagnosis of gout: an accuracy and diagnostic yield study. Ann Rheum Dis 2015, 74:1072–1077. [PubMed: 24671771]
71. Dalbeth N, House ME, Aati O, Tan P, Franklin C, Horne A, Gamble GD, Stamp LK, Doyle AJ, McQueen FM: Urate crystal deposition in asymptomatic hyperuricaemia and symptomatic gout: a dual energy CT study. Ann Rheum Dis 2015, 74:908–911. [PubMed: 25637002]
72. Glazebrook KN, Guimaraes LS, Murthy NS, Black DF, Bongartz T, Manek NJ, Leng S, Fletcher JG, McCollough CH: Identification of intraarticular and periarticular uric acid crystals with dual-energy CT: initial evaluation. Radiology 2011, 261:516–524. [PubMed: 21926378]
73. Jia E, Zhu J, Huang W, Chen X, Li J: Dual-energy computed tomography has limited diagnostic sensitivity for short-term gout. 2018:773–777.
74. Baer AN, Kurano T, Thakur UJ, Thawait GK, Fuld MK, Maynard JW, Mcadams-demarco M, Fishman EK, Carrino JA: Dual-energy computed tomography has limited sensitivity for non-tophaceous gout : a comparison study with tophaceous gout. BMC Musculoskeletal Disorders 2016:1–9. [PubMed: 26728594]
75. Löckmann V, Veit-haibach P, Schmid L, Kantonsspital L, Kantonsspital L: Difficult diagnosis of gout : clinical practice on commercial use on l co m on er al. 2013, 5:50–53.
76. Melzer R, Pauli C, Treumann T, Krauss B: Gout tophus detection — A comparison of dual-energy CT (DECT) and histology. Seminars in Arthritis and Rheumatism 2014, 43:662–665. [PubMed: 24332008]
77. Huppertz A, Geert K, Diekhoff T, Wagner M, Hamm B, Schmidt WA: Systemic staging for urate crystal deposits with dual - energy CT and ultrasound in patients with suspected gout. 2014:763–771.
78. Lu H, Sheng J, Dai J, Hu X: Tophaceous gout causing lumbar stenosis. 2017, 32:32–35.
79. Pottecher P, Martz P, Ornetti P: Paraparesis Revealing Tophaceous Gout. Arthritis & rheumatology (Hoboken, N.J.) 2018, 70:942.
80. Alqatari S, Visevic R, Marshall N, Ryan J, Murphy G: An unexpected cause of sacroiliitis in a patient with gout and chronic psoriasis with inflammatory arthritis : a case report. 2018:18–20.
81. Barazani S, Chi W, Pyzik R, Jacobi A, Donnell TO, Fayad Z: Detection of Uric Acid Crystals in the Vasculature of Patients with Gout Using Dual-Energy Computed Tomography.1–3.
82. Carr A, Doyle AJ, Dalbeth N, Mcqueen FM, Carr A, Aj D, Dalbeth N, Aati O, Fm M: Deposits in Costal Cartilage and. 2016:1063–1067.
83. Kiefer T, Diekhoff T, Hermann S, Stroux A, Mews J, Blobel J, Hamm B, Hermann K-gA: Single source dual-energy computed tomography in the diagnosis of gout : Diagnostic reliability in comparison to digital radiography and conventional computed tomography of the feet. European Journal of Radiology 2016, 85:1829–1834. [PubMed: 27666624]
84. Tanikawa H, Ogawa R, Okuma K, Harato K, Niki Y, Kobayashi S: Detection of calcium pyrophosphate dihydrate crystals in knee meniscus by dual-energy computed tomography. 2018:1–6.
85. Kim H-r, Lee J-h, Kim NR, Lee S-h: Detection of calcium pyrophosphate dihydrate crystal deposition disease by dual-energy computed tomography. 2014:404–405.
86. Diekhoff T, Kiefer T, Stroux A, Pilhofer I, Juran R, Mews J, Blobel J, Tsuyuki M, Ackermann B, Hamm B, et al.: Detection and Characterization of Crystal Suspensions Using. 2015, 50:255–260.

Key points:

- Delay in synovial fluid analysis up to three days does not hinder crystal detection.
- MSU and CPP crystal detection by CPLM remains challenging even by highly motivated and trained individuals.
- Novel methods for crystal detection are being developed that may enable point-of-care diagnosis.
- US and DECT are highly specific for crystal deposition.
- Sensitivity of US and DECT to detect urate deposition is dependent on duration and burden of disease.

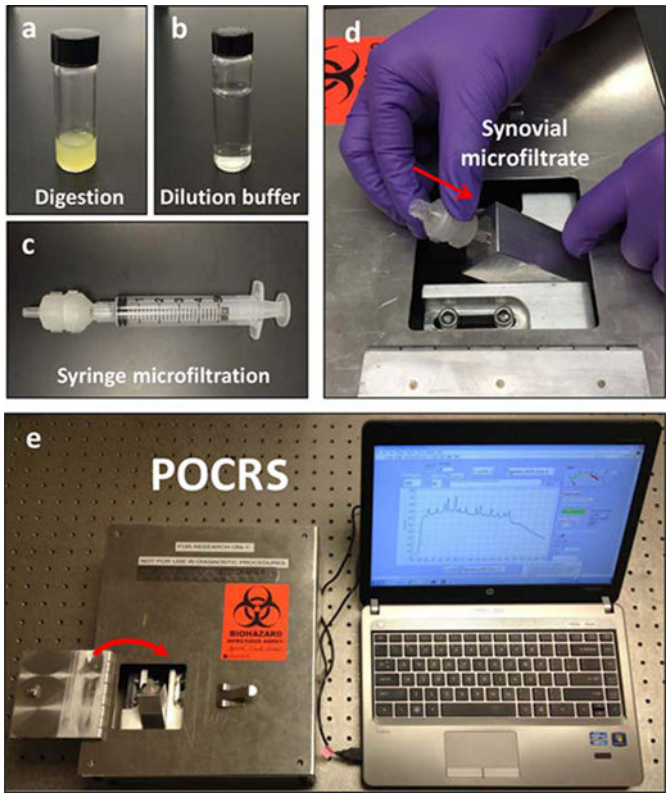

Figure 1: Point-of-care Raman spectroscopy.

The point-of-care Raman spectroscopy (POCRS) system consists of 2 parts: a syringe microfiltration kit for isolating and collecting arthritic crystals from synovial fluid (a–c) and a shoebox-sized optoelectromechanical system for acquiring diagnostic signals (d and e). To use the system, synovial fluid is loaded in a glass vial with digestive enzymes (a). After 30 minutes of digestion at 408C, the uric acid–supplemented buffer (b) is used to dilute the digested synovial fluid. Following dilution, the synovial fluid is transferred into a standard syringe (c) and pushed through the disposable microfiltration cartridge for crystal collection. After microfiltration, the cartridge is directly inserted into the optoelectromechanical system (d) for diagnostic signal acquisition (e).

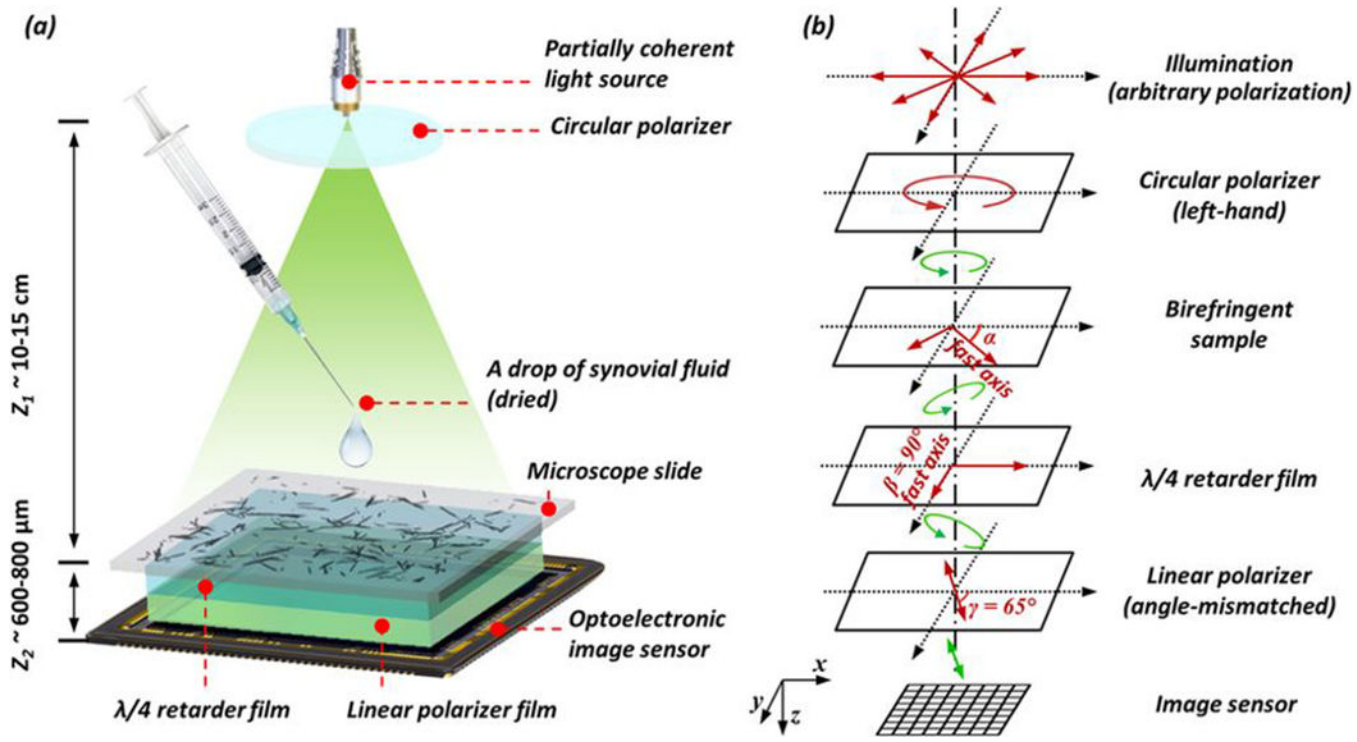

Figure 2: Schematic set-up of lens-free polarized microscopy.

(**a**) Schematic setup of lens-free differential holographic polarized microscopy. (**b**) Design of the polarization in this system. The light, which is propagating from top to bottom, passes through a left-hand circular polarizer, the birefringent sample, a λ/4 retarder film, a linear polarizer and reaches the image sensor. The orientations of the polarizing components are illustrated with red arrows, and the polarization states of the light between components are illustrated with green arrows.

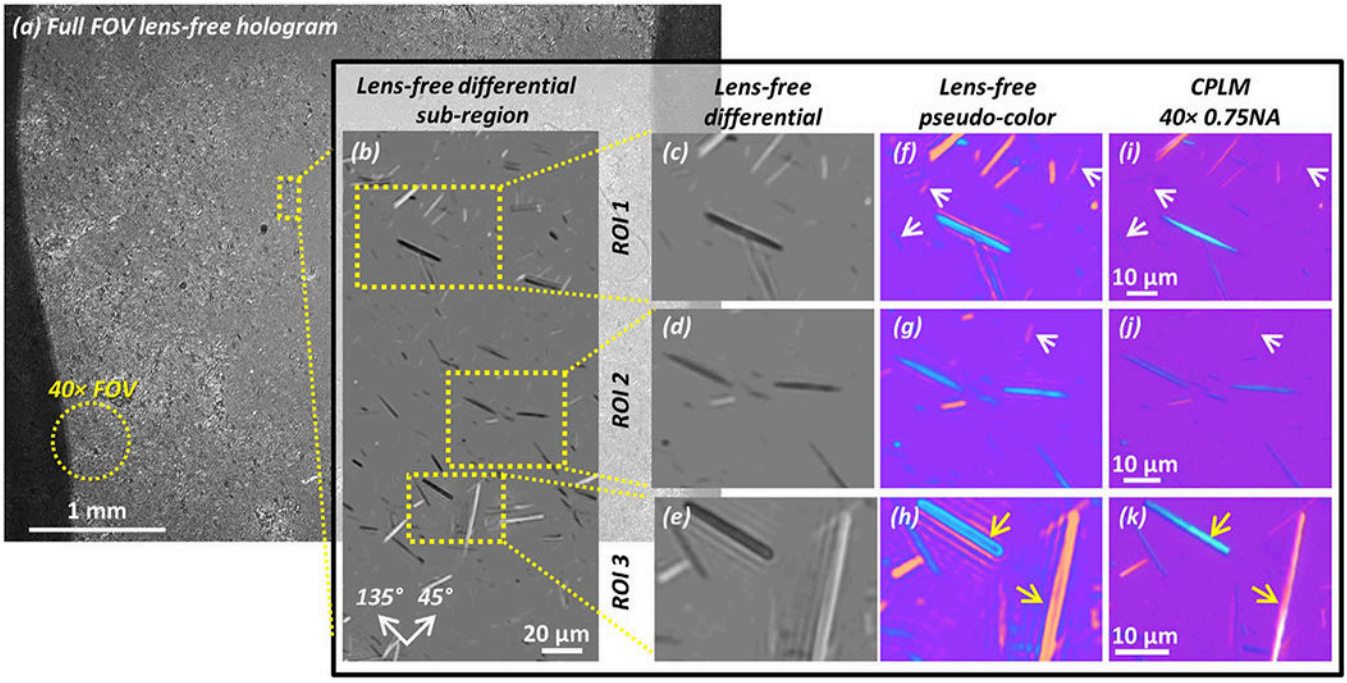

Figure 3: High-resolution wide-field of view images of monosodium urate crystals using lens-free microscopy.

(**a**) The full FOV of the lens-free polarized image is 20.5 mm^2 , approximately 2 orders of magnitude larger than the FOV of a typical 40×microscope objective lens (see yellow dashed circle). (**b**) A sub-region showing the lens-free polarized image. Crystals oriented along the 45° axis (see orientation guide in the bottom left) appear brighter than the background, and those along the 135° axis appear darker. (**c–e**) Lens-free grayscale differential image of 3 ROIs taken from (**b**). (**f–h**) Pseudo-colored images of (**c–e**) to approximate familiar CPLM images. (**i–k**) 40×0.75 numerical aperture CPLM images of the same regions as (**f–h**). White arrows: crystals that result in a weak signature have better contrast in the lens-free pseudo-color images (**f,g**) than the CPLM images (**i,j**). Yellow arrows: thick MSU crystals in the lens-free pseudo-color image (**h**) have hollow appearances, slightly different from the CPLM image (**k**).

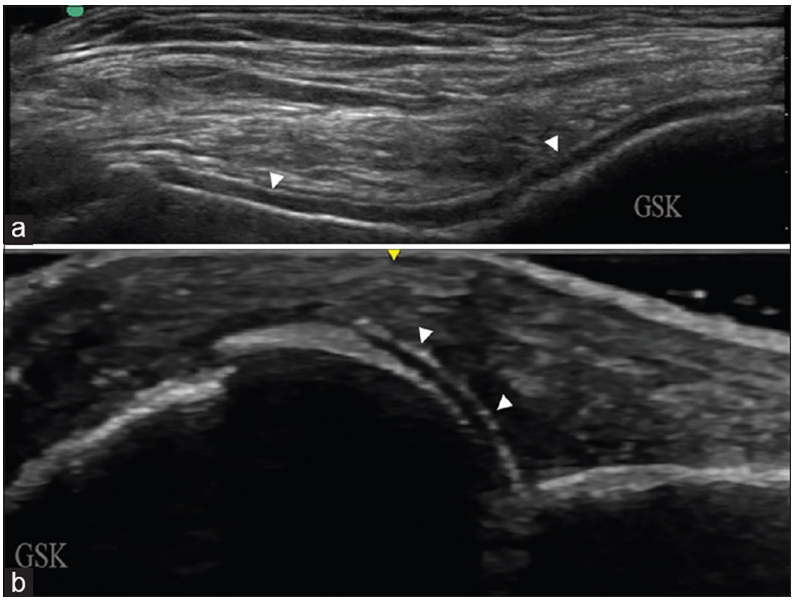

Figure 4: Ultrasound image of double contour sign

(a) Double contour sign at the femoral condyle (arrowheads). (b) Double contour sign (arrowheads) at the metacarpophalangeal joint.

Figure 5: Dual energy CT 3D image and quantification of monosodium urate deposition

Dual-energy computed tomography with three-dimensional reconstruction of the bilateral feet showing large green color mapping areas involving multiple joints, tendons, and soft tissue suggestive of monosodium urate crystals forming tophi. Approximate volume: 13.46 cm^3